Proceedings of the 9th World Congress on Mechanical, Chemical, and Material Engineering (MCM'23)
Brunel University, London, United Kingdom - August 06-08, 2023
Paper No. ICMIE 131
DOI: 10.11159/icmie23.131

Application Limits of small dimensioned Sintered Journal Bearings in Grease-lubricated Planetary Gears

Luis Huber[1], Alexander Monz[2]
[1,2]Nuremberg Institute of Technology
Keßlerplatz 12, 90489 Nuremberg, Germany
[1]luis.huber@th-nuernberg.de; [2]alexander.monz@th-nuernberg.de

Abstract – The design of machine elements as sintered components offers further potential in addition to economic advantages in production and technical innovations, such as the use of self-lubricating components. As a result, sintered planetary gears are now being used in planetary gear units, with a journal bearing bushing integrated in the bore. In this context, it is necessary both to consider the material requirements in the joint material selection and to optimally resolve controversial design variables of both, the gear and the journal bearing, such as the gear width and the journal bearing width. On the occasion of this trend in development, the present research work deals with the application limits of sintered planetary journal bearings under grease lubrication. In the field of drive technology, it can be observed that these cannot be designed reliably according to the usual design guidelines, such as DIN 31652 1-4, VDI 2204 1-4 or ISO 7902 1-3 for conventional journal bearings. The result is failure of the bearing due to seizure and wear. Therefore, the decisive parameters need to be determined and further analysed. Due to the mutual influence on the operating performance of journal bearing and gearing and the resulting large number of parameters sets, it is not promising to systematically optimize the journal bearing system in gearbox tests. Therefore, the influence of the planetary gear is first abstracted. On a test bench specially developed for this application, the operating behaviour of a journal bearing bushing rotating around a stationary shaft is mapped and tested analogously to the operating conditions in a planetary gear. In the project, characteristic diagrams are thus generated for the characterization of sintered journal bearings. The results obtained by varying the parameter sets are presented and discussed.

Keywords**:** Journal Bearing, Planetary Gear, Sinter, Hydrodynamic, Grease Lubrication, Testing

1. Introduction

Journal bearings allow low-friction movement between shaft and bushing in the ideal operating range (So = 1 - 10). In hydrodynamic journal bearings, a lubricant such as oil or grease is used to separate the two components without contact by maintaining a sufficient relative velocity. In the majority of applications, the shaft rotates in a stationary bushing. Since journal bearings are increasingly used in planetary gearboxes, the rotating bushing is now the focus of attention. Furthermore, the reduction of the installation space is becoming increasingly important, which is why the bearings are often designed very compactly (outer diameter $d \leq 10$ mm). Based on these considerations, a test rig has been developed on which journal bearings of small size are investigated with varying lubrication condition and rotating bushing.

2. State of Art

Hydrodynamic radial journal bearings separate shaft and bushing by the hydrodynamic pressure build-up in the lubricant. Basic calculation methods for operationally reliable design are provided by DIN 31652 [1], [2], VDI 2204 [3], [4] and ISO 7902 [5], [6].

Prölß [7] extends the simulation tool CombrosR by an approach for the calculation of slow-running and highly loaded planetary gear bearings. Hagemann et al [8] use a thermohydrodynamic model to analyse the influence of the helix angle of the gearing on the journal bearings in planetary gears and the edge bearing that occurs as a result. Suitable countermeasures are defined here as the selection of a robust lubricant and axial crowning of the sliding surface. Guo et al [9] consider the load distribution of planetary gears with journal bearings and conclude that it is distributed more evenly by increasing the bearing clearance or the torque applied to the gear.

Susilowati et al [10] and Cui et al [11] investigate the properties of self-lubricating, sintered sliding materials by varying the mass ratios of the alloying elements and determine an ideal value with regard to the mechanical and tribological

properties. Neacşu et al [12] experimentally validate a simulation to determine the Stribeck curve of sintered journal bearings and achieve a high rate of correlation between experimental results and simulation.

Kumada [13] presents the influence of circumferential micro-grooves on the running surfaces of journal bearing bushings. It is revealed that these reduce the heating of the journal bearing due to the increased convection surface. Furthermore, it is shown that the service life is significantly longer after the lubricant supply is interrupted, since residual oil is still present in the microgrooves. Tala-Ighil [14] numerically investigates the effect of textured bushing surfaces on the sliding properties. Ideal texture areas for the respective operating conditions are explained. Partial texturing in the falling pressure zone is explicitly recommended, which locally increases the lubricant film thickness and thus reduces the friction in the journal bearing, as well as exerting a positive effect on the cavitation zone. The influence of misalignment on the performance of journal bearings is described in detail by Bouyer and Fillon [15]. It is generally shown that the effects of misalignment are greater the lower the speed, as consequently the counteracting hydrodynamic forces are also lower.

Maintenance-free ceramic journal bearings are extensively investigated by Stentzel [16]. Based on numerical and experimental findings, a design suitable for ceramic journal bearings is formulated. The application range of water-lubricated plastic journal bearings is divided by Ginzburg [17] into three stress-dependent groups, to which preferred plastics are assigned. Amann et al [18] investigate galvanically coupled journal bearings to minimise friction and determine that by coupling water with complex fluids, a significant reduction in friction and wear can be achieved compared to conventional oil lubrication. Lu and Khonsari [19] carry out tribometer tests on oil- and grease-lubricated journal bearings and conclude that grease is better suited for highly loaded journal bearings in the area of boundary and mixed friction than in liquid friction, as it has a lower coefficient of friction here compared to oil.

3. Test Bench

In a planetary gear with a stationary ring gear, the planet and shaft rotate in opposite directions, resulting in a relative velocity $v_{relative}$, which is derived from the absolute value of the circumferential velocities of planet v_{planet} and shaft v_{shaft}, see Fig. 1. Since the relative velocity is ultimately decisive for journal bearings, a stationary shaft is assumed in the following, around which the bushing rotates with the relative velocity $v_{relative}$. This makes it possible to assume a constant load direction, since it rotates synchronously with the shaft speed. This simplifies the development of an application-oriented test bench which, in contrast to conventional journal bearing test benches, includes a rotating bushing instead of a rotating shaft. The effects of the rotating planet carrier on the lubricant are not considered.

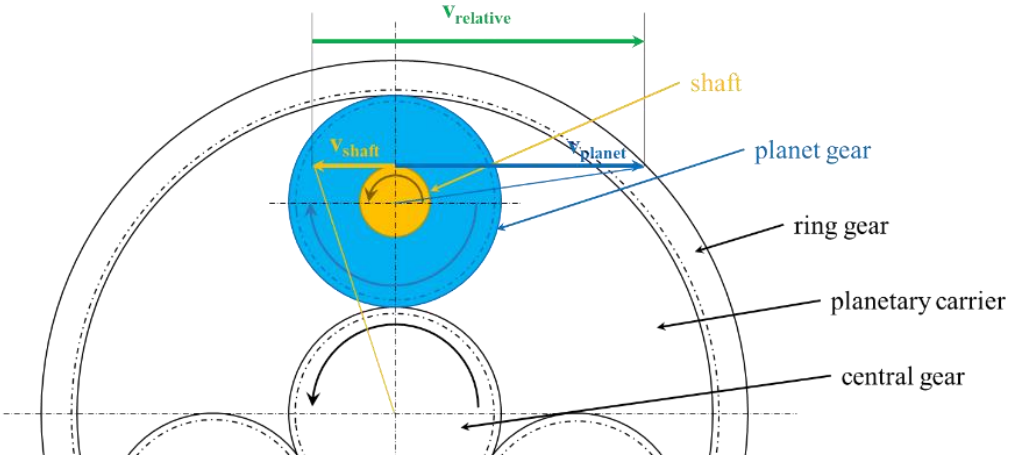

Fig. 1: Velocity ratios in a planetary gear with stationary ring gear and driving central gear

On the test bench at Nuremberg Institute of Technology, see Fig. 2, the test wheel is mounted in a tool spindle by means of a chuck and driven by an electric motor. The radial load is applied from the opposite side, where a likewise clamped test shaft is inserted into the bore of the test bushing by means of a slide. This test shaft is vertically adjustable and thus enables the journal bearing position to be loaded by applying weights via a defined lever arm. Both test specimens are located in a sealed oil pan which, in addition to the planned grease lubrication, also allows test operation under oil sump or oil injection lubrication. In addition to the variation of the lubrication condition and the operating point, the test bench also allows geometrical adjustments, such as a change in the bearing width, the bearing clearance, or a successive adjustment of the bearing diameter.

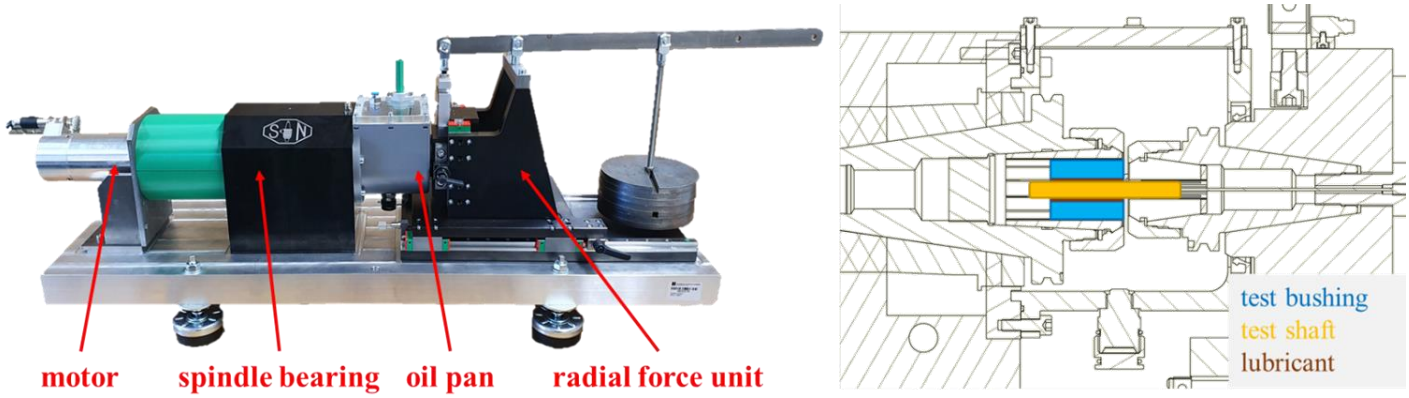

Fig. 2: Journal bearing test bench at Nuremberg Institute of Technology (left) and sectional view of its oil pan (right)

On the test bench shown, the motor speed and current are read out during the test run by means of an internal encoder. A force sensor attached to the lever arm determines the radial load on the journal bearing. The temperature in the test specimen, in the oil sump and in the environment are recorded using thermocouples. A multimeter determines the electrical resistance between the test wheel and the test shaft in order to make a qualitative statement about the surface contact of the two friction partners.

Table 1: Overview of the measuring equipment used on the journal bearing test bench

Measuring equipment	Measured variable	Unit	Maximum value	Accuracy
Encoder	Speed	min-1	4,000	0.14 %
	Current	A	36	0.14 %
Forcer Sensor	Radial force	N	1,000	10
Thermocouple	Environmental temperature	K	453	1
	Oil pan temperature	K	453	1
	Test specimen temperature	K	453	1
Multimeter	Electrical Resistance	Ω	10^15	0.015 %

4. Test Method

To evaluate the operating conditions, a characteristic diagram of the surface pressure p versus the circumferential velocitiy v (PV diagram) is generated for each variant by means of experimental tests. The product of these two quantities is the PV value. It is generally used to characterize the heat input in the journal bearing and to assess its service life. [16], [20]

$$PV = p \cdot v \tag{1}$$

The map tests are carried out with the same geometry (d/w=8 mm/22 mm). Rolling elements made of 100Cr6 are used as the shaft, which have a narrow tolerance zone. This results in a similar geometry in terms of diameter and shape. The bushings are made of SintD32. These are sintered, which means that the diameter and shape of the bore have comparable sizes. The operating parameters rotational speed and radial force define the operating points shown in the characteristic diagram and are varied between the individual operating points. In preliminary tests, a characteristic test duration of eight hours was determined. After this test period has elapsed, or after a failure has occurred, the test run is stopped and the damage pattern is then examined. In many cases, a conspicuous behaviour in the measurement curves of the test specimen temperature and the motor current is already apparent in the first hours, whereby a conclusion can be drawn about the further operating behaviour. This allows a large number of operating points to be validated in a short time. Repeated tests ensure the validity of the test results. In order to be able to qualitatively assess the test results, the tests are divided into three damage categories after reviewing the tested specimens and the associated measurement data:

Good – test shaft shows light, even material removal on the contact surface

Wear – test shaft shows heavy, uneven material removal on the contact surface

Failure – jamming between test shaft and test bushing

Exemplary damage patterns for the damage categories "Good", "wear" and "failure" are shown in Fig. 3. The running surfaces of exemplary test shafts are shown here. The black markings on the outside indicate the course of the line load which significantly stresses the stationary test shaft. The image for failure illustrates a test shaft that has already been detached from the test bushing and shows foreign bodies on the surface.

Fig. 3: Illustration of the three damage categories "Good" (top), "Wear" (middle) and "Failure" (bottom)

In this project, characteristic maps are investigated with two grease lubricants of NLGI class 2 with comparable viscosity but contrary chemical attributes. Their properties are compared in Table 2.

Table 2: Properties of lubricating greases

Characteristics	Grease A	Grease B
Base oil	Polyalphaolefin (PAO)	Paraffinic base oil
thickener used	Polyurethane	Polyurea
NLGI class (acc. DIN 51818)	2	2
Base oil viscosity 40 °C	100 mm²/s	115 mm²/s
Base oil viscosity 100 °C	15.3 mm²/s	12.2 mm²/s
contains solid lubricant (Y/N)	Y	N

5. Evaluation

The test results with grease A and grease B are shown in Fig. 4. The boundaries between the individual damage forms can be characterised by constant PV values. These boundaries are confirmed for further points along the hyperbolas by further test results. A damage category is only confirmed when it has been proven in at least two individual tests. If different damage categories occur when determining an operating point, these are represented in the diagram.

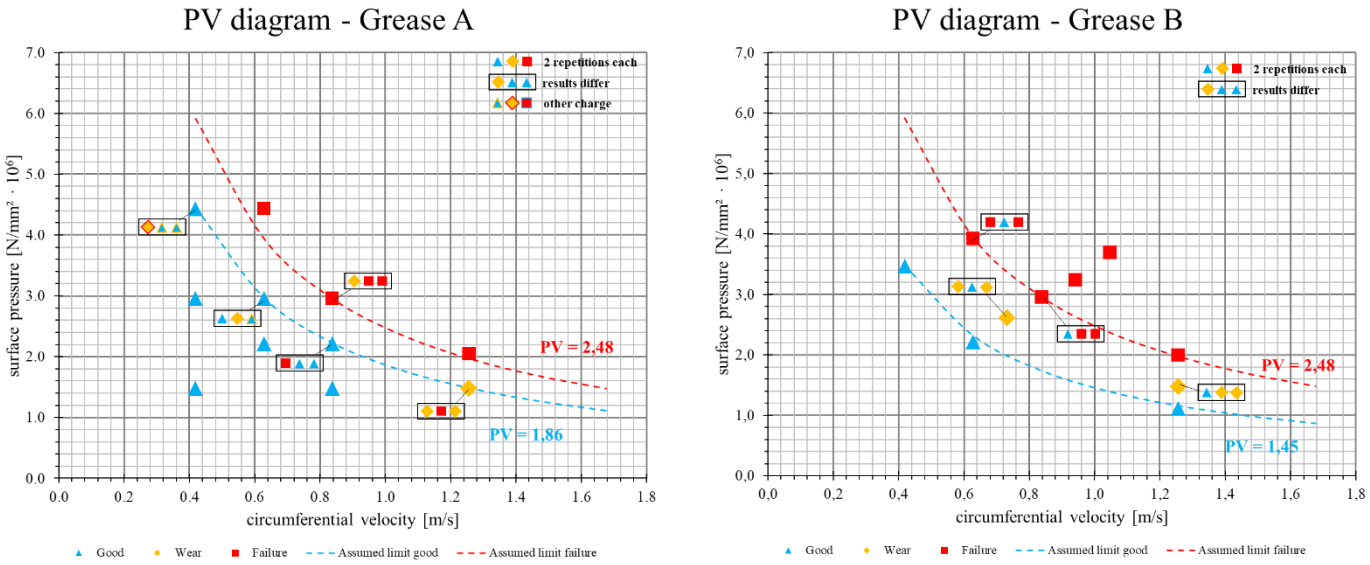

Fig. 4: PV diagrams of the tested specimens (left: Grease A, right: Grease B)

For both greases, a clear demarcation of the damage categories for specific PV values is shown in Table 3. These differ only in the assumed limit in the transition from "good" to "wear" at a PV value of 1.86 · 106 N/ms for grease A and 1.45 · 106 N/ms for grease B. Furthermore, it can be observed that operating points which are closer to boundary transition tend to cause different damage categories more frequently. This observation gives reason to determine further operating points in the limit range in order to improve the informative value of the maps.

Table 3: PV value at the transition of the damage categories

Transition	Unit	PV value Grease A	PV value Grease B
Good to Wear	N/ms	$1.86 \cdot 10^6$	$1.45 \cdot 10^6$
Wear to Failure	N/ms	$2.48 \cdot 10^6$	$2.48 \cdot 10^6$

6. Damage Analysis

The test specimens show a very distinct, repetitive damage pattern of the damage category " Failure". The test shaft and the test bushing are tightly jammed together and can neither be loosened axially nor rotated into each other. When cutting open the corresponding test specimens, a conspicuous damage to the test shaft can be seen. This shows a material increase in the central area of the running surface, see Fig. 5. The running surface of the test bushing indicates that progressive damage has occurred here, as strong circumferential scoring can be seen at the level of the material increase. It can be concluded from this that adhesive damage to the journal bearing has taken place in the form of scuffing.

Fig. 5: Scuffing damage on test bushing (top) and test shaft (bottom)

The SEM examination in Fig. 6 show that alloy components of the test bushing can be detected in the foreign material of the test shaft. It consists of 0.86 % molybdenum and has hardly any chromium at 0.01 %. The test bush is made of SintD32, whose molybdenum content is between 0.6% and 2% according to DIN 30910-4 [21], but it does not contain any chromium. Accordingly, it is proven that adhesive damage in the form of scuffing damage occurs here.

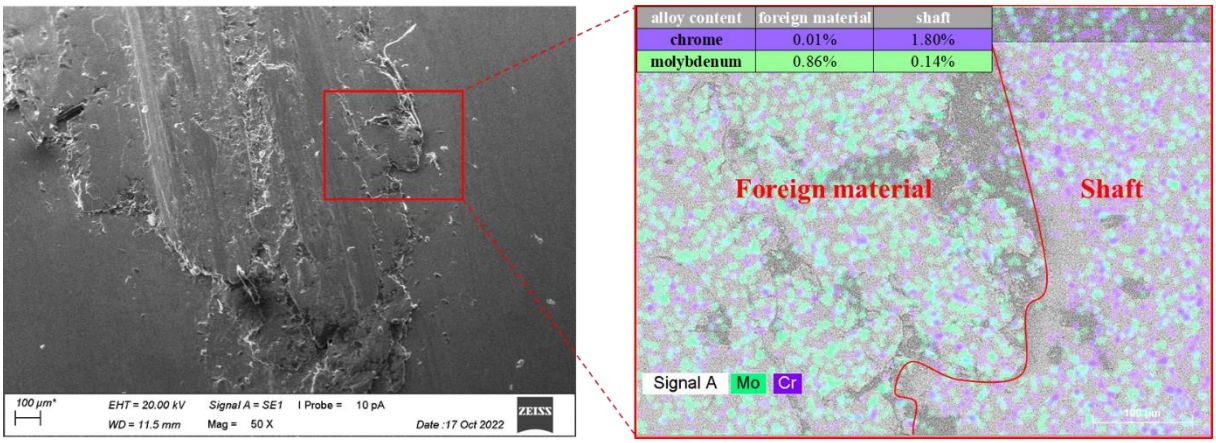

Fig. 6: SEM analysis of the scuffing damage of the test shaft

7. Conclusion

In the course of the test series, two characteristic maps were generated with different grease lubricants. The following findings were obtained:

1) Characteristic maps were generated for two different greases. The limit values of the PV value for adhesive damage in the considered journal bearing were determined at $2.48 \cdot 10^6$ N/ms for both examined greases. Different results for one operating point can be obtained more frequently in the boundary transition of two damage categories.

2) The failure of the journal bearings is indicated by a jamming between the test shaft and the test bushing. The components can neither be moved axially to each other nor rotate in opposite directions. The journal bearing is no longer operational due to scuffing damage. This damage can already be observed within the first eight hours of the test.

3) During the process of scuffing damage, there is a transfer of material from the bushing to the shaft. This can be confirmed by means of SEM examination by detecting foreign material on the shaft, that contains alloy elements of the bushing.

8. Acknowledgements

The project was funded by the Bavarian State Government under the Program for the Promotion of Applied Research and Development.

References

[1] ‘DIN 31652-1:2017-01, Gleitlager_- Hydrodynamische Radial-Gleitlager im stationären Betrieb_- Teil_1: Berechnung von Kreiszylinderlagern’, Beuth Verlag GmbH. doi: 10.31030/2588236.

[2] ‘DIN 31652-3:2017-01, Gleitlager_- Hydrodynamische Radial-Gleitlager im stationären Betrieb_- Teil_3: Betriebsrichtwerte für die Berechnung von Kreiszylinderlagern’, Beuth Verlag GmbH. doi: 10.31030/2588238.

[3] ‘VDI 2204-1:1992-09, Auslegung von Gleitlagerungen - Grundlagen’, Beuth Verlag GmbH.

[4] ‘VDI 2204-2:1992-09, Auslegung von Gleitlagerungen - Berechnung’, Beuth Verlag GmbH.

[5] ‘ISO 7902-1:2020(E) Hydrodynamic plain journal bearings under steady-state conditions - Circular cylindrical bearings - Part 1: Calculation procedure’.

[6] ‘ISO 7902-3:2020(E) Hydrodynamic plain journal bearings under steady-state conditions - Circular cylindrical bearings - Part 3: Permissible operational parameters’.

[7] M. Prölß, ‘Berechnung langsam laufender und hoch belasteter Gleitlager in Planetengetrieben unter Mischreibung, Verschleiß und Deformation’, Technische Universität Clausthal, Clausthal, 2020.

[8] T. Hagemann, H. Ding, E. Radtke, and H. Schwarze, ‘Operating Behavior of Sliding Planet Gear Bearings for Wind Turbine Gearbox Applications—Part I: Basic Relations’, *Lubricants*, vol. 9, no. 10, Art. no. 10, Oct. 2021, doi: 10.3390/lubricants9100097.

[9] Z. Guo, S. Li, W. Wu, and L. Zhang, ‘Quasi-Static Load Sharing Characteristics of a Planetary Gear Set with Planet Journal Bearings’, *Applied Sciences*, vol. 10, no. 3, Art. no. 3, Jan. 2020, doi: 10.3390/app10031113.

[10] S. E. Susilowati, A. Fudholi, and D. Sumardiyanto, ‘Mechanical and microstructural characteristics of Cu–Sn–Zn/ Gr metal matrix composites processed by powder metallurgy for bearing materials’, *Results in Engineering*, vol. 14, p. 100377, Jun. 2022, doi: 10.1016/j.rineng.2022.100377.

[11] G. Cui, M. Niu, S. Zhu, J. Yang, and Q. Bi, ‘Dry-Sliding Tribological Properties of Bronze–Graphite Composites’, *Tribol Lett*, vol. 48, no. 2, pp. 111–122, Nov. 2012, doi: 10.1007/s11249-012-0007-8.

[12] I. A. Neacşu, B. Scheichl, G. Vorlaufer, S. J. Eder, F. Franek, and L. Ramonat, ‘Experimental Validation of the Simulated Steady-State Behavior of Porous Journal Bearings1’, *Journal of Tribology*, vol. 138, no. 3, Apr. 2016, doi: 10.1115/1.4032659.

[13] Y. Kumada, K. Hashizume, and Y. Kimura, ‘Performance of Plain Bearings with Circumferential Microgrooves’, *Tribology Transactions*, vol. 39, no. 1, pp. 81–86, Jan. 1996, doi: 10.1080/10402009608983505.

[14] N. Tala-Ighil, ‘Effect of textured area on the performances of a hydrodynamic journal bearing | Elsevier Enhanced Reader’. https://reader.elsevier.com/reader/sd/pii/S0301679X10002379?token=E88C7C010BE8FE0B708DA7F9ADC2AD015F9A9230F8FA0191C3141B9A2EA62B8055CAE2D36FD638657479DDD52DA528E5&originRegion=eu-west-1&originCreation=20230313131525 (accessed Mar. 13, 2023).

[15] J. Bouyer and M. Fillon, ‘An Experimental Analysis of Misalignment Effects on Hydrodynamic Plain Journal Bearing Performances’, *Journal of Tribology*, vol. 124, no. 2, pp. 313–319, Jul. 2001, doi: 10.1115/1.1402180.

[16] C. Stentzel, ‘Entwicklung wartungsfreier und rein elastisch beanspruchter Gleitlager auf Basis keramischer Werkstoffe’, Technische Universität Dresden, Dresden, 2019.

[17] B. M. Ginzburg, D. G. Tochil’nikov, V. E. Bakhareva, A. V. Anisimov, and O. F. Kireenko, ‘Polymeric materials for water-lubricated plain bearings’, *Russ J Appl Chem*, vol. 79, no. 5, pp. 695–706, May 2006, doi: 10.1134/S1070427206050016.

[18] T. Amann, W. Chen, M. Baur, A. Kailer, and J. Rühe, ‘Entwicklung von galvanisch gekoppelten Gleitlagern zur Reduzierung von Reibung und Verschleiß’, *Forsch Ingenieurwes*, vol. 84, no. 4, pp. 315–322, Dec. 2020, doi: 10.1007/s10010-020-00416-z.

[19] X. Lu and M. M. Khonsari, ‘An Experimental Investigation of Grease-Lubricated Journal Bearings’, *Journal of Tribology*, vol. 129, no. 1, pp. 84–90, Oct. 2006, doi: 10.1115/1.2401216.

[20] H. Czichos and K.-H. Habig, *Tribologie-Handbuch*. Wiesbaden: Vieweg+Teubner, 2010. doi: 10.1007/978-3-8348-9660-5.

[21] ‘DIN 30910-4:2010-03, Sintermetalle_- Werkstoff-Leistungsblätter (WLB)_- Teil_4: Sintermetalle für Formteile’, Beuth Verlag GmbH. doi: 10.31030/1561175.